

Exo2EgoSyn: Unlocking Foundation Video Generation Models for **Exocentric-to-Egocentric Video Synthesis**

Mohammad Mahdi¹ Yuqian Fu^{1*} Nedko Savov¹ Jiancheng Pan¹ Danda Pani Paudel¹ Luc Van Gool¹ ¹INSAIT, Sofia University "St. Kliment Ohridski"

Abstract

Foundation video generation models such as WAN 2.2 exhibit strong text- and image-conditioned synthesis abilities but remain constrained to the same-view generation setting. In this work, we introduce Exo2EgoSyn, an adaptation of WAN 2.2 that unlocks Exocentric-to-Egocentric (Exo2Ego) cross-view video synthesis. Our framework consists of three key modules. Ego-Exo View Alignment (EgoExo-Align) enforces latent-space alignment between exocentric and egocentric first-frame representations, reorienting the generative space from the given exo view toward the ego view. Multi-view Exocentric Video Conditioning (MultiExoCon) aggregates multi-view exocentric videos into a unified conditioning signal, extending WAN 2.2 beyond its vanilla single-image or text conditioning. Furthermore, Pose-Aware Latent Injection (PoseInj) injects relative exo-to-ego camera pose information into the latent state, guiding geometry-aware synthesis across viewpoints. Together, these modules enable high-fidelity egoview video generation from third-person observations without retraining from scratch. Experiments on ExoEgo4D validate that Exo2EgoSyn significantly improves Ego2Exo synthesis, paving the way for scalable cross-view video generation with foundation models. Source code and models will be released publicly.

1. Introduction

Exocentric-to-egocentric (Exo2Ego) cross-view video generation aims to synthesize how the world would appear from a first-person viewpoint given a third-person observation of the same scene, with promising applications in robotics, augmented reality, and virtual reality. This task requires not only transferring the visual perspective but also inferring fine-grained spatial and temporal cues, such as body dynamics and hand-object interactions, and recovering details

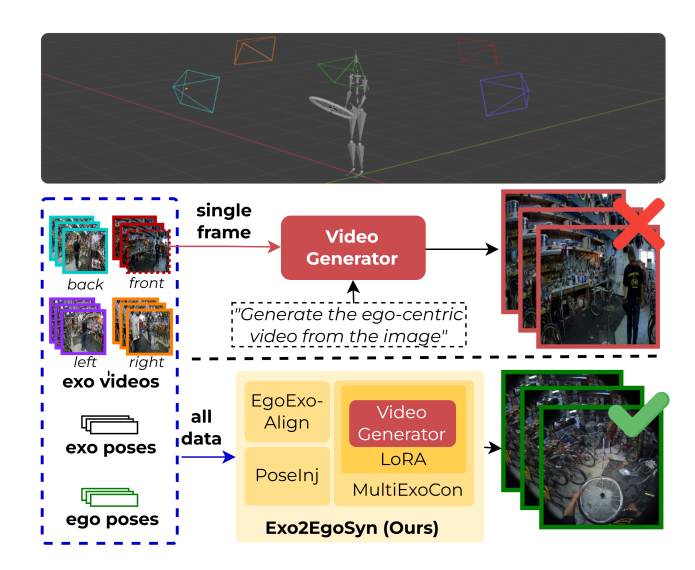


Figure 1. Adapting a video generator for Exo2Ego task with ExoEgoSyn. Top: Multi-view (4 exo, 1 ego) setup. Middle: The original generator cannot perform cross-view translation. Bottom: Our model ExoEgoSyn enables exo2ego cross-view translation.

that are only partially observable from exocentric views, making it a challenging and largely unsolved problem.

Few efforts [32, 36, 41, 52] have been made to address this task; however, most existing approaches design tasktailored models and train them from scratch on cross-view paired videos, typically from Ego-Exo4D [11]. The limited training source inevitably restricts their generalization ability. In contrast, a number of emerging foundation video generation models, e.g., WAN2.2 [49], trained on largescale and diverse video corpora with strong generalization even under zero-shot settings. Yet, these foundation models are inherently designed for single-view generation, leaving their potential adaptation to cross-view scenarios largely unexplored. This gap motivates a central question: Can we unlock the capability of current foundation video generation models for cross-view scenarios, particularly for the Exo2Ego video generation task?

^{*}Corresponding author.

To achieve this, we must address two key obstacles: ① **Strong view bias.** Foundation video generation models are trained on massive datasets consisting of individual videos, which leads to inherent view biases. More specifically, when conditioned on an image, such models tend to reproduce subsequent frames from the same viewpoint or camera pose as the conditioning image, as in Fig. 1. This behavior conflicts with the cross-view generation setup, where the target video should begin from a different viewpoint rather than the conditioned one. ② Limited conditioning support. Most existing foundation models allow video generation conditioned on text descriptions or a single image, leaving novel conditioning signals, such as multi-view exocentric observations or camera poses, unexplored. Although prior works [1, 2] have explored incorporating new conditioning types, they typically assume access to a model already fine-tuned on its standard conditions (e.g., text), which is not the case in our scenario.

In this work, we start from WAN2.2, one of the most recent, flagship, and high-performing video generation models, and use it as an example to tackle the Exo2Ego video generation task by addressing the two aforementioned challenges. Specifically, to tackle ①, we note that the first frame, which serves as the sole image condition, plays a crucial role in determining the viewpoint or camera space of the generated video. Instead of avoiding this inherent bias, we propose to leverage it to facilitate Exo2Ego translation. To this end, we introduce an Ego-Exo View Alignment (EgoExo-Align) module, which enforces alignment between the latent representations of the first frames from the ego- and exocentric videos. Although seemingly straightforward, this design effectively guides the model to shift its generation space from the exocentric to the egocentric view. Furthermore, to fully exploit the available information in the Exo2Ego video generation task, we condition the model on multiple exocentric videos and known camera poses. For this purpose, we propose two additional components: Multi-view Exocentric Video Conditioning (MultiExoCon) and Pose-Aware Latent Injection (PoseInj), both addressing ②. In particular, MultiExoCon is implemented by replacing the original supported text tokens with video latent tokens from the exocentric videos, while PoseInj is integrated into the network by first lifting its sparse representation into a dense form and then combining it with the hidden state of the Diffusion, bridging the gap between sparse pose information and dense feature representations. Notably, we focus on the relative pose between the exocentric and egocentric views, which naturally aligns with the objective of the Exo2Ego translation task.

Formally, with all the newly proposed modules integrated into the vanilla WAN2.2, we present a novel framework, termed **Exo2EgoSyn**, for exocentric-to-egocentric video generation. To the best of our knowledge, this is

the first approach that successfully explores and extends a single-view foundation video generation model to crossview generation tasks, thereby broadening its applicability and generalization capability. Extensive experiments on the challenging Ego-Exo4D benchmark show that Exo2EgoSyn consistently advances beyond the proposed baseline, delivering substantial performance improvements on this task.

In summary, our contributions are threefold: 1) We present Exo2EgoSyn, the first framework that extends a single-view foundation video generation model to the exocentric-to-egocentric video generation task. 2) We design three key modules, including EgoExo-Align, Multi-ExoCon, and PoseInj, enabling effective view translation and multi-video, pose-aware conditioning. 3) Extensive experiments on the Ego-Exo4D benchmark show that our approach outperforms the baseline, delivering clear performance gains.

2. Related Works

2.1. Ego-exo Cross-view Learning

The recent release of ego–exo dual-view datasets [11, 22], particularly Ego-Exo4D [11], opens new opportunities for enabling cross-view understanding. For example, Ego-Exo Object Correspondence [9, 10, 38, 40] focuses on associating objects of the same identity across views through segmentation-based matching, while Ego-Exo Video Question Answering (VQA) [14, 29] aims to jointly reason over ego- and exocentric videos for holistic video understanding. In this paper, we target Ego-Exo Video Generation [32], a more challenging direction that goes beyond perception and understanding to synthesis.

Despite its importance, this task has been relatively underexplored, with only a few recent attempts. Luo et al. [37] learn to generate egocentric videos from exocentric inputs by first predicting hand trajectories, while EgoWorld [41] reconstructs egocentric views from exocentric depth, 3D hand poses, and textual cues through point-cloud reprojection and diffusion-based inpainting. EgoExo-Gen [52] further leverages action text and the first egocentric frame to guide egocentric video synthesis from exocentric observations. Intention-driven generation [36] explores the inverse direction, generating exocentric videos from egocentric inputs using motion trajectories and cross-view conditioning. Most related to our work, Exo2Ego-V [32] integrates multiple exocentric views and camera poses within a PixelNeRF-based diffusion framework with temporal attention for exocentric-to-egocentric video generation. In this work, we follow the basic setting of Exo2Ego-V, which does not rely on ground-truth ego signals, e.g., the first frame, but only uses multiple exocentric views and ego/exo camera poses. Crucially, in contrast to prior models that train from scratch or with a limited video source, we are the

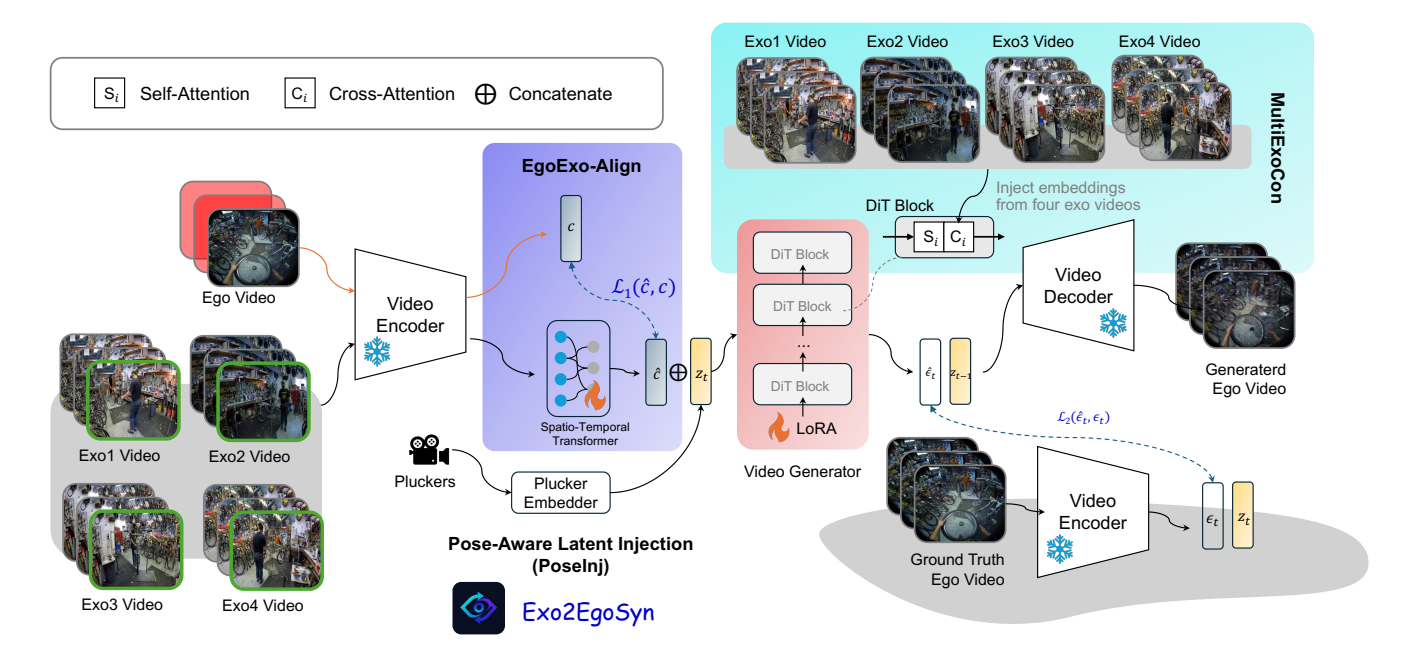


Figure 2. **Exo2EgoSyn Framework.** We first propose the EgoExo-Align module, which predicts the latent representation of the first frame of the ego video. The MultiExoCon module replaces the original text conditioning in the foundation model with latent tokens derived from exocentric videos, injected into each DiT block of the diffusion model. During the second stage of fine-tuning, we concatenate the Plücker embeddings of the relative camera poses with the hidden states of the diffusion model before passing them to the first DiT block.

first to tackle this task from the perspective of adapting a large-scale pretrained video foundation model.

Recent advances have extended image diffusion models [21, 34, 35, 39, 44] to video editing [31, 43, 51] and generation [5, 16, 18, 55, 56]. Tune-A-Video [51] adapts image diffusion via cross-frame attention to transfer motion between videos, while Video Diffusion Models [18] employ a factorized space-time U-Net for video synthesis. Stable Video Diffusion [4] improves quality through large-scale data curation, and AnimateDiff [12] introduces a motion module for text-to-image animation; similar architectures have been applied to human image animation [20, 53]. However, despite these advances and strong image-generation capabilities [8, 15, 17, 47], the potential of diffusion models for cross-view video generation remains largely unexplored. Besides, most video diffusion systems are conditioned on text or a single image, with recent progress driven by Diffusion Transformers (DiTs) [42, 54]. Although additional signals such as camera poses can, in principle, be incorporated [3, 13, 23, 25–27, 30, 33, 48, 50], existing methods typically rely on backbones pretrained or fine-tuned for these specific inputs [1, 2, 24]. Yet, to the best of our knowledge, no pretrained foundation model currently supports either multi-view exocentric videos or relative exo2ego camera poses which are important for building a robust Exo2Ego generator. These gaps motivate exploring whether foundation video generation models, taking the most recent and well-performed WAN2.2 as an example,

can be *adapted* for Exo2Ego generation, under novel conditioning signals.

3. Methodology

3.1. Preliminaries

Video Latent Diffusion Models. A video Latent Diffusion Model (LDM) operates by transforming an input video into a compact latent representation through a pretrained Variational Auto-Encoder (VAE). The diffusion process is performed entirely in this latent space, where the model learns to iteratively denoise a noisy latent variable to recover a clean and coherent representation. The resulting latent is then decoded by the VAE back into the video space, yielding the final output sequence.

The employed VAE applies a spatiotemporal compression with factors $(c_f, c_h, c_w) \in \mathbb{N}^3$ along the temporal and spatial dimensions, respectively, effectively reducing the number of frames by a factor of c_f and spatial resolution by (c_h, c_w) . This latent-space formulation enables efficient training and inference while preserving high-fidelity video generation.

WAN2.2 Baseline. WAN2.2 is a powerful foundational video LDM designed for high-quality video generation conditioned on text and/or images. It employs a 3D Variational Auto-Encoder (VAE) with a temporal compression factor $c_f \neq 1$, meaning that motion across every c_f consecutive frames is encoded into a single latent frame. Throughout

this paper we show the temporal dimension in RGB and latent space by F and f respectively, where $f=\frac{F}{c_f}$. We follow the same notation for spatial dimensions where H and W defines the height and width in RGB space and $h=\frac{H}{c_h}$ and $w=\frac{W}{c_m}$ for latent spatial dimension.

The diffusion model component of WAN2.2 performs denoising on the video latents using a sequence of Diffusion-Transformer (DiT) blocks. Each block applies a self-attention operation over the latent video tokens, followed by a cross-attention operation between the latent video tokens and the text tokens. Image conditioning is achieved by zero-padding the input image along the temporal dimension to match the number of frames in RGB space, encoding it with the same VAE, and concatenating its latent representation with the noisy video latent. Although this architecture is, in principle, capable of handling video-conditioned generation, the pretrained WAN2.2 model has not been trained on video conditions.

3.2. Framework Overview

Task Definition. Given four exocentric videos $V^{\text{exo}} =$ $\{V_1^{\rm exo}, V_2^{\rm exo}, V_3^{\rm exo}, V_4^{\rm exo}\}$ of shape $4\times F\times C\times H\times W$, captured by fixed cameras arranged 360° around daily-life skilled human activities, our goal is to generate the corresponding egocentric video $V^{\text{ego}} \in \mathbb{R}^{F \times C \times H \times W}$. To model both the environment and camera motions, the model is to be conditioned on both video content and camera poses. Let the fixed exocentric camera poses be $\mathcal{P}^{\text{exo}} =$ $\{P_1^{\mathrm{exo}}, P_2^{\mathrm{exo}}, P_3^{\mathrm{exo}}, P_4^{\mathrm{exo}}\}$, where each $P_i^{\mathrm{exo}} \in \mathbb{R}^{4 \times 4}$, and let the egocentric camera poses be $\mathcal{P}^{\mathrm{ego}} = \{P_t^{\mathrm{ego}}\}_{t=1}^F$, which vary across frames. We define the relative camera pose between the egocentric frame at time t and a reference exocentric camera (chosen here as the first camera) as $P_t^{\text{rel}} = (P_t^{\text{ego}})^{-1} P_1^{\text{exo}}$. This formulation enables the model to jointly condition on multi-view exocentric information and temporal camera motion when generating the egocentric video.

This task is particularly challenging due to the combined effects of environmental complexity and camera motion, especially in scenarios such as bike repair. Additionally, not all exocentric views are equally informative, as some cameras may capture the operator from suboptimal angles. Therefore, the model must selectively integrate information from multiple views.

Our Framework. To address this problem, we propose *Exo2EgoSyn*, a multi-video and camera-pose conditioned latent diffusion model that adapts the pretrained WAN2.2 model for cross-view video generation. This task is challenging for two main reasons: first, the pretrained model exhibits a bias to replicate the conditioned image as the first frame of the generated video, which complicates cross-view generation; second, WAN2.2 has not been trained on video conditions or camera poses, and its original text-based con-

ditioning is not applicable to our setting. To overcome these challenges, Exo2EgoSyn proposes a Ego-Exo View Alignment (EgoExo-Align), followed by a two-stage finetuning strategy on WAN2.2, which uses Multi-view Exocentric Video Conditioning (MultiExoCon) and Pose-Aware Latent Injection (PoseInj) to enable conditioning the model on multiple exo videos and relative camera poses we have, respectively. The overall framework is shown in Fig. 2

3.3. EgoExo-Align Module

The EgoExo-Align module is a transformer model with the purpose of predicting the latent representation of the first egocentric frame, given the latent of the first frame of each exocentric video V_i^{exo} and the ego-exo Plücker-embedded relative camera poses. This component proved crucial, as it bypasses the tendency of the video generator to replicate the starting frame in the generated video. This effect was observed even when Wan2.2 was conditioned on a video (Sup.Mat.) and even when prompted to produce the egocentric video (demonstrated in Fig. 1). Finetuning the model proved ineffective, as the pretrained weights are already biased towards this behavior. In contrast, by conditioning on the frame, predicted by our EgoExo-Align module, the video generator is able to predict a video with the correct viewpoint.

The EgoExo-Align module is defined as follows:

$$\hat{l}_1^{\text{rego}} = \phi\Big(x: \left[vae(\mathcal{V}_{i,1}^{\text{exo}})\right]_{i=1}^4, \ y: \left[E(P_{t=1}^{rel^i}, K)\right]_{i=1}^4\Big),$$

where $vae(\cdot)$ denotes the pretrained VAE, $\mathcal{V}_{i,1}^{\mathrm{exo}}$ represents the first frame of the i-th exocentric video, $P_{t=1}^{rel^i}$ defines the relative pose of the first frame of the i-th exocentric view, and $E(\cdot)$ applies the Plücker representation to the sparse relative poses, providing 6D per-pixel geometry-aware features given the egocentric camera intrinsic parameters K. We employ STTransformer [6], as implemented by [45], denoted by ϕ . It interleaves spatial-temporal blocks, each of which first performs attention across the height and width of the images (spatial), then across all frames (temporal). (details in Sup.Mat.) In our case, the four exocentric frames form the temporal channels.

3.4. Relaxing Novel Conditions

As discussed earlier, our task requires a model capable of conditioning not only on a single video, but simultaneously on four videos. Moreover, the model must integrate camera poses as an additional conditioning signal. The mismatch between WAN2.2's original capabilities and these requirements poses a substantial challenge. To address this, we introduce a two-stage finetuning approach: where we first handle four exocentric video conditioning using our Multi-ExoCon, and then address camera pose guidance via applying our PoseInj.

3.4.1. Multi-view Exocentric Video Conditioning

In the WAN2.2 model, each block first applies a selfattention operation over the video latent tokens, followed by a cross-attention operation with the text tokens. To enable multi-view video conditioning, we replace the text input with our four exocentric videos and train only the crossattention modules of WAN2.2. Additionally, we employ LoRA to finetune the self-attention layers, allowing efficient adaptation to the multi-video input.

To achieve this, we first collect the VAE-encoded latents corresponding to each exocentric video, resulting in a signal of shape $(f, 4*c_{\dim}, h, w)$. We then apply a patch embedding function ψ , implemented as a 3D convolution with kernel size and stride of (1,2,2), an input channel dimension of $4*c_{\dim}$, and an output channel dimension matching the hidden state size of the self-attention module (c_m) . This operation transforms the latents into a tensor of shape $(f, c_m, \frac{h}{2}, \frac{w}{2})$. Next, we build a token sequence of length $\frac{f*h*w}{4}$, with each token represented by a vector of dimension c_m , which we denote as \mathbf{X}_{toks} :

$$\mathbf{X}_{\text{toks}} = \text{flatten}\Big(\psi\Big([vae(\mathcal{V}_1^{\text{exo}})]_{i=0}^4\Big)\Big),$$

where $flatten(\cdot)$ is the flattening operator to produce the token sequence. These tokens are then fed into the crossattention module to update the hidden states h:

$$\mathbf{h} \leftarrow \mathbf{h} + CA(\mathbf{X}_{toks}, \mathbf{h}).$$

Importantly, in this stage, the output of $\phi(\cdot)$ consistently serves as the conditioning input to the diffusion model.

3.4.2. Pose-Aware Latent Injection

Sherwin et al. [2] demonstrate that camera-pose information constitutes a low-frequency signal that can easily be overlooked by large DiT-based diffusion models. Consequently, simply injecting pose information into an intermediate layer is insufficient for effective conditioning. Following the approach of [1], we first convert the sparse relative camera poses into a dense per-pixel representation, given the intrinsic matrix (K) of the ego camera. This is achieved using Plücker representation, which encode each pixel with a 6-dimensional feature vector uniquely defining a 3D ray. The resulting tensor has shape $(F \times 6 \times H \times W)$.

The Plücker embeddings are computed for each frame, yielding F representations, whereas WAN2.2 operates on a temporally compressed latent space, where every four consecutive frames are encoded into a single latent ($c_f=4$). As a result, the raw Plücker coordinates cannot be directly incorporated into the model. While one could naively downsample or reshape the pose sequence to match the latent resolution, this approach would inefficiently merge motion information across the four-frame window.

Instead, following [1], we apply a sequence of causal 1D convolutions to transform the $F \times 6$ Plücker coordinate sequence for each pixel into a $(f \times 96)$ representation for each 8×8 spatial grid. This produces a tensor of shape $f \times 96 \times H/8 \times W/8$, which is then concatenated to the hidden state prior to entering the first DiT block of WAN2.2. We observe that the pretrained weights obtained from the multi-video cross-attention finetuning stage facilitate effective conditioning on camera poses in this step. Since the camera-pose features are fed into the DiT blocks, we also employ LoRA finetuning for the self-attention modules to adapt them to the pose-conditioned input. We highlight that, although pose embeddings have been explored in prior work, this is the first time they are introduced into the Exo2Ego generation task, through a natural and effective modification that embeds relative exo-to-ego camera poses.

3.5. Training and Loss Functions

We first train the ExoEgoAlign module, minimizing

$$\mathcal{L}_1 = \left\| l_1^{\text{ego}} - \hat{l}_1^{\text{ego}} \right\|_1,$$

and use the detached produced latents as the condition to WAN2.2. We then train the cross-attention layers with the video tokens from the four exocentric videos. We apply LoRA finetuning to the self-attention layers, allowing the model to leverage motion information directly induced by the video frames to better adapt the target egocentric frames. Specifically, we optimize the diffusion objective:

$$\mathcal{L}_2 = \left\| \epsilon_t - \mathcal{W} \left([z_t, \hat{l}_1^{\mathrm{ego}}], \mathcal{V}^{\mathrm{exo}}, t \right) \right\|^2,$$

where z denotes the noisy latent input, W indicates the WAN2.2 diffusion model, t is the timestep, and ϵ is the ground-truth noise applied in the forward diffusion process.

In the second stage, we initialize the model with the weights obtained from the previous stage and concatenate the Plücker embeddings to the hidden state before feeding it into the sequence of DiT blocks. During this stage, we LoRA finetune the self-attention modules and optimize the following loss:

$$\mathcal{L}' = \left\| \epsilon_t - \mathcal{W}([z_t, \hat{l}_1^{\text{ego}}, E(P^{rel}, K)], \mathcal{V}^{\text{exo}}, t) \right\|^2.$$

Each stage is trained for 100k steps on 2×NVIDIA H200 GPUs, with a training time of around 10 hours. Further details on model size, training configurations, and hyperparameters are provided in the Sup.Mat.

4. Experiments

4.1. Experimental Setup

Dataset. We evaluate our approach on four categories of the Ego-Exo4D [11] benchmark: Bike, Basketball, Covid Test,

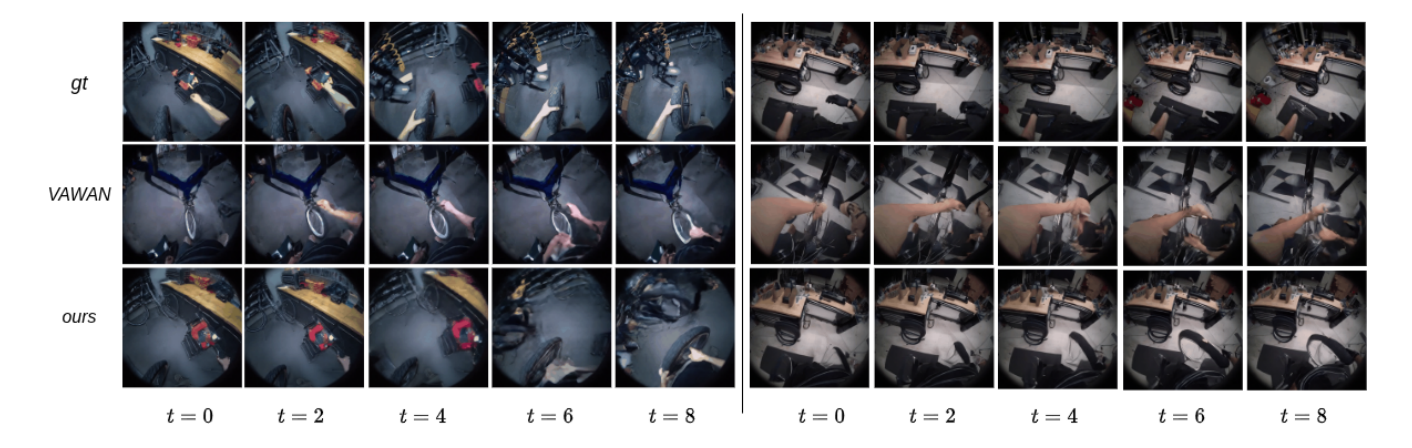


Figure 3. **Qualitative Results.** On the left, a scene with high camera motion is shown, while on the right, a more complex environment is selected to illustrate our model's capabilities across different scenarios.

Category	PSNR↑	SSIM↑	LPIPS↓
Bike			
VAWAN	14.8511	0.3709	0.5289
Ours	15.1319	0.3895	0.5052
Basketball			
VAWAN	15.9996	0.4768	0.4989
Ours	16.6445	0.5052	0.4158
CPR			
VAWAN	15.2329	0.4935	0.5249
Ours	16.7229	0.5294	0.4096
Covid			
VAWAN	14.0127	0.3889	0.5974
Ours	14.4812	0.4312	0.4868

Table 1. **Comparison results.** Exo2EgoSyn Results Compared to the Baseline VAWAN.

and CPR. For each egocentric video, the dataset provides four exocentric videos along with the corresponding camera poses for the fixed exocentric cameras and for every frame of the egocentric video. Additionally, the intrinsic parameters of the egocentric camera are provided, which we utilize in the Plücker embedding computation. Our experiments process 363 videos from the Bike category, 910 videos from Basketball, 246 videos from Covid Test, and 98 videos from CPR. Both egocentric and exocentric videos are spatially resized to a resolution of H=W=256. Since the WAN2.2

architecture requires the number of frames to satisfy 4n+1, we sample 9 frames per video. Using a skip-frame step of 4 during preprocessing ensures sufficient motion is captured in the sampled frames. For training and testing splits, we follow the official partitions released by [11].

Baseline Construction. As discussed in Section 3.1, the WAN2.2 natively supports video-shaped inputs, since it zero-pads the conditioned image to match the temporal dimension. Leveraging this capability, we introduce a baseline, *Video-Accepting WAN (VAWAN)*, for our experiments. In VAWAN, the model is conditioned on four exocentric videos by generalizing the standard image-conditioning mechanism: rather than conditioning on a single frame, we concatenate the VAE-encoded latents of all four exocentric videos along the channel dimension and integrate them with the noisy input latent, preserving the original architectural design. To incorporate camera motion, we evaluate both raw camera poses and dense Plücker embeddings under various configurations, as detailed in our ablation study.

Evaluation Metrics. To quantitatively evaluate our method, we assess performance using PSNR, SSIM, and LPIPS (AlexNet [28]), following the evaluation protocol outlined in [32] to ensure a consistent and fair comparison with the baseline. However, because these metrics do not fully capture the perceptual quality of generative outputs, we additionally conduct a user study. A total of 100 video samples—25 from each category—are evaluated by human participants, who compare the outputs of our model against those of the baseline. More details about user study is provided in the Sup.Mat.

4.2. Comparison with Baseline

As summarized in Table 1, our model consistently outperforms VAWAN across all four categories, with particularly notable gains in SSIM and LPIPS. On average, we observe

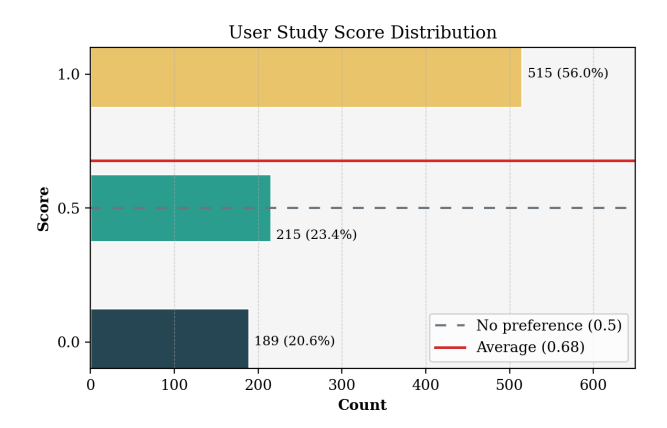


Figure 4. **User Study Score Distribution.** A clear preference to our model (score 1) is noticed, compared to the lower preference votes for baseline (score 0) or no preference (score 0.5).

an approximate 10% improvement in SSIM and a 16% reduction in LPIPS, indicating substantial enhancements in perceptual quality. See qualitative results in Fig. 3.

To further demonstrate the effectiveness of our pipeline, we conducted a complementary user study with 10 participants, following the design of [46]. Scoring is based on the ground truth similarity of our model's outputs against those of the baseline VAWAN, in terms of hand-object interaction, camera motion and visual fidelity. The scoring options are preference for ours (1.0), for the baseline (0.0), or no preference (0.5). Fig. 4 shows the preference distribution, indicating a clear preference for our model, also confirmed by a final average score of **0.68**.

4.3. Ablation Studies

We perform an ablation study to evaluate the contributions of different components in our pipeline. Specifically, we investigate the presence and architectural variations of the ExoEgo-Align module. We also assess the role of the proposed PoseInj module during the second stage of finetuning. Finally, we examine the impact of the number of exocentric views and various camera-pose conditionings.

EgoExo-Align Module. As shown in Table 2, we ablate the presence of the EgoExo-Align module and also establish an upper bound for its performance by directly using the first frame of the target ego video. We observe that removing this module leads to a notable degradation in performance. All experiments are conducted with the proposed MultiExoCon module, but excluding the PoseInj module, to isolate and evaluate the effect of EgoExo-Align.

As shown in Table 3, we further ablate the effectiveness of different architectures used to implement the EgoExo-Align module, with the STTransformer achieving the most

	Scenario		Bike	
		PSNR↑	SSIM↑	LPIPS↓
	+EgoExo-Align	15.0216	0.3798	0.5101
MultiExoCon	-EgoExo-Align	14.7361	0.3450	0.5359
	+GT frame	15.5327	0.4321	0.3951

Table 2. **EgoExo-Align Existence.** *GT Frame* refers to conditioning the model directly on the first frame of the ground-truth ego video, providing an upper-bound performance for our proposed module.

Base	Arc	Pose		Bike	
			PSNR↑	SSIM↑	LPIPS↓
	Cross-Attn	N	14.1216	0.3342	0.5988
	Cross-Attn	Y	14.2902	0.3391	0.5773
VAWAN	Pixel-Nerf	Y	14.5223	0.3301	0.5944
	${\bf ST\text{-}Transformer}^S$	Y	14.5387	0.3529	0.5470
	${\bf ST\text{-}Transformer}^L$	Y	14.7227	0.3630	0.5320

Table 3. **EgoExo-Align Architecture.** The *Cross-Attn* model uses convolutional layers to encode the input frames, and the applies a cross-attention module between these merged encodings and the camera-pose embeddings. We use the pretrained *Pixel-Nerf* models for different categories from [32]. The superscripts S and L indicate the size of the spatiotemporal transformer: the small version (S) has 4 heads, 4 blocks, and a dimension of 128, while the large version (L) has 8 heads, 8 blocks, and a dimension of 512.

promising results. For these experiments, we use the proposed baseline, VAWAN, under various camera-pose conditioning scenarios. When active, camera poses are embedded into the model depending on the architecture; specifically, the STTransformer leverages the Plücker coordinates of the relative camera poses from the first frames of each exocentric video.

PoseInj Module. As illustrated in Table 4, we conduct an extensive ablation on the presence of the PoseInj component during the second fine-tuning step across all categories of the Ego-Exo4D dataset. The results demonstrate the robustness of the proposed module across different experimental setups.

Exo Views. We ablate the number of exocentric videos used for generation. As expected, and shown in Table 5, due to the limited training data compared to what the WAN 2.2 model was trained on, training the full model can lead to overfitting. Furthermore, increasing the number of exocentric videos generally improves performance, since some

Category	ours w/o PoseInj				ours	
	PSNR↑	SSIM↑	LPIPS↓	PSNR↑	SSIM↑	LPIPS↓
Bike (gt-frame)	15.5327	0.4321	0.3951	15.5862	0.4326	0.3881
Bike	15.0216	0.3798	0.5101	15.1319	0.3895	0.5052
Basketball	16.3158	0.4901	0.4299	16.6445	0.5052	0.4158
CPR	15.9145	0.4617	0.4308	16.7229	0.5294	0.4096
Covid	14.0823	0.4091	0.5103	14.4812	0.4312	0.4868

Table 4. **PoseInj Presence.** *gt-frame* indicates that the ExoEgo-Align module is not used, and the model is directly conditioned on the first frame of the target ego video.

Scenario	V	Training	Bike		
			PSNR↑	SSIM↑	LPIPS↓
	1	LoRA	14.5278	0.3375	0.5821
VAWAN-AC3D	4	LoRA	14.8511	0.3709	0.5289
	4	Whole	14.5101	0.3305	0.5971

Table 5. **Number of Exo Views Used.** When using 1 exo video, we randomly choose between 4 available views.

VAWAN gt-frame					
Pose cond	V	PSNR↑	SSIM↑	LPIPS↓	
Time&Pose	1	14.2125	0.3252	0.5944	
AC3D (512)	1	15.2965	0.4350	0.4027	
AC3D (512)	4	15.2524	0.4346	0.4057	
AC3D (512) Shared	4	15.1409	0.4298	0.4169	
AC3D (2048)	4	15.3268	0.4368	0.4026	

Table 6. **Camera Conditioning.** *Time & Pose* is adapted from [32], where timesteps and camera-pose information are first fused before being input to the diffusion model. The numbers in parentheses (\cdot) indicate the bottleneck dimension of the additional DiT blocks proposed in [2].

videos may be captured from suboptimal angles. Here, we incorporate the pose-conditioning approach proposed in [2] into our baseline model.

Camera Conditioning We have already ablated the presence of the PoseInj component in the second part. Here, as shown in Table 6, we investigate different strategies

for camera-pose conditioning, following the approaches of [32] and [2]. The former uses a UNet-based architecture and fuses information between timesteps and camera poses, while the latter introduces additional DiT blocks, applying an attention mechanism between compressed latent representations and camera poses in a lower-dimensional space. We ablate different bottleneck dimensions for this compression and also evaluate a variant in which the newly added DiT blocks are shared across all main DiT blocks of WAN2.2.

5. Conclusion

We propose a novel framework to adapt strong foundational video generation models to the Exo2Ego cross-view translation task. Specifically, we build on WAN2.2, a powerful video Latent Diffusion Model designed for text- and imageconditioned video generation. Our task presents two key challenges: (1) breaking biases learned by the foundation model when finetuning with limited data, and (2) aligning the conditioning input with the model's expected format. To address the first, we introduce EgoExo-Align, which predicts the latent of the target ego frame from the first frames of multiple exocentric views, bypassing the model's tendency to replicate the conditioned input. For the second, we employ a two-stage adaptation: the first stage conditions WAN2.2 on all exocentric videos to provide informative cues about future ego frames by use of the MultiExo-Con, while the second stage enhances camera-tracking by incorporating Plücker embeddings of relative camera poses into the hidden state before the DiT blocks, using PoseInj module. We also introduce a baseline, Video-Accepting WAN (VAWAN), that extends WAN2.2 to accept multivideo conditions and explore different camera-pose conditioning scenarios. Our quantitative and qualitative evaluations on the challenging subcategories of the Ego-Exo4D dataset demonstrate the robustness of our approach over the VAWAN baseline model.

References

- [1] Sherwin Bahmani, Ivan Skorokhodov, Aliaksandr Siarohin, Willi Menapace, Guocheng Qian, Michael Vasilkovsky, Hsin-Ying Lee, Chaoyang Wang, Jiaxu Zou, Andrea Tagliasacchi, et al. Vd3d: Taming large video diffusion transformers for 3d camera control. *arXiv preprint* arXiv:2407.12781, 2024. 2, 3, 5
- [2] Sherwin Bahmani, Ivan Skorokhodov, Guocheng Qian, Aliaksandr Siarohin, Willi Menapace, Andrea Tagliasacchi, David B Lindell, and Sergey Tulyakov. Ac3d: Analyzing and improving 3d camera control in video diffusion transformers. In *Proceedings of the Computer Vision and Pattern Recognition Conference*, pages 22875–22889, 2025. 2, 3, 5, 8
- [3] Jianhong Bai, Menghan Xia, Xiao Fu, Xintao Wang, Lianrui Mu, Jinwen Cao, Zuozhu Liu, Haoji Hu, Xiang Bai, Pengfei Wan, et al. Recammaster: Camera-controlled generative rendering from a single video. arXiv preprint arXiv:2503.11647, 2025. 3
- [4] Andreas Blattmann, Tim Dockhorn, Sumith Kulal, Daniel Mendelevitch, Maciej Kilian, Dominik Lorenz, Yam Levi, Zion English, Vikram Voleti, Adam Letts, et al. Stable video diffusion: Scaling latent video diffusion models to large datasets. arXiv preprint arXiv:2311.15127, 2023. 3, 16
- [5] Andreas Blattmann, Robin Rombach, Huan Ling, Tim Dockhorn, Seung Wook Kim, Sanja Fidler, and Karsten Kreis. Align your latents: High-resolution video synthesis with latent diffusion models. In *Proceedings of the IEEE/CVF conference on computer vision and pattern recognition*, pages 22563–22575, 2023. 3
- [6] Jake Bruce, Michael D Dennis, Ashley Edwards, Jack Parker-Holder, Yuge Shi, Edward Hughes, Matthew Lai, Aditi Mavalankar, Richie Steigerwald, Chris Apps, et al. Genie: Generative interactive environments. In Forty-first International Conference on Machine Learning, 2024. 4, 12
- [7] Xiangxiang Chu, Zhi Tian, Bo Zhang, Xinlong Wang, and Chunhua Shen. Conditional positional encodings for vision transformers. arXiv preprint arXiv:2102.10882, 2021. 13
- [8] Prafulla Dhariwal and Alexander Nichol. Diffusion models beat gans on image synthesis. *Advances in neural information processing systems*, 34:8780–8794, 2021. 3
- [9] Yuqian Fu, Runze Wang, Yanwei Fu, Danda Pani Paudel, and Luc Van Gool. Cross-view multi-modal segmentation@ egoexo4d challenges 2025. arXiv preprint arXiv:2506.05856, 2025. 2
- [10] Yuqian Fu, Runze Wang, Bin Ren, Guolei Sun, Biao Gong, Yanwei Fu, Danda Pani Paudel, Xuanjing Huang, and Luc Van Gool. Objectrelator: Enabling cross-view object relation understanding across ego-centric and exo-centric perspectives. In *Proceedings of the IEEE/CVF International* Conference on Computer Vision, pages 6530–6540, 2025. 2
- [11] Kristen Grauman, Andrew Westbury, Lorenzo Torresani, Kris Kitani, Jitendra Malik, Triantafyllos Afouras, Kumar Ashutosh, Vijay Baiyya, Siddhant Bansal, Bikram Boote, et al. Ego-exo4d: Understanding skilled human activity from first-and third-person perspectives. In *Proceedings of*

- the IEEE/CVF Conference on Computer Vision and Pattern Recognition, pages 19383–19400, 2024. 1, 2, 5, 6
- [12] Yuwei Guo, Ceyuan Yang, Anyi Rao, Zhengyang Liang, Yaohui Wang, Yu Qiao, Maneesh Agrawala, Dahua Lin, and Bo Dai. Animatediff: Animate your personalized textto-image diffusion models without specific tuning. arXiv preprint arXiv:2307.04725, 2023. 3
- [13] Hao He, Yinghao Xu, Yuwei Guo, Gordon Wetzstein, Bo Dai, Hongsheng Li, and Ceyuan Yang. Cameractrl: Enabling camera control for video diffusion models. In *The Thirteenth International Conference on Learning Representations*, 2025. 3
- [14] Yuping He, Yifei Huang, Guo Chen, Baoqi Pei, Jilan Xu, Tong Lu, and Jiangmiao Pang. Egoexobench: A benchmark for first-and third-person view video understanding in mllms. arXiv preprint arXiv:2507.18342, 2025. 2
- [15] Jonathan Ho, Ajay Jain, and Pieter Abbeel. Denoising diffusion probabilistic models. *Advances in neural information processing systems*, 33:6840–6851, 2020. 3
- [16] Jonathan Ho, William Chan, Chitwan Saharia, Jay Whang, Ruiqi Gao, Alexey Gritsenko, Diederik P Kingma, Ben Poole, Mohammad Norouzi, David J Fleet, et al. Imagen video: High definition video generation with diffusion models. arXiv preprint arXiv:2210.02303, 2022. 3
- [17] Jonathan Ho, Chitwan Saharia, William Chan, David J Fleet, Mohammad Norouzi, and Tim Salimans. Cascaded diffusion models for high fidelity image generation. *Journal of Machine Learning Research*, 23(47):1–33, 2022. 3
- [18] Jonathan Ho, Tim Salimans, Alexey Gritsenko, William Chan, Mohammad Norouzi, and David J Fleet. Video diffusion models. *Advances in neural information processing systems*, 35:8633–8646, 2022. 3
- [19] Edward J Hu, Yelong Shen, Phillip Wallis, Zeyuan Allen-Zhu, Yuanzhi Li, Shean Wang, Lu Wang, and Weizhu Chen. LoRA: Low-rank adaptation of large language models. In *International Conference on Learning Representations*, 2022.
- [20] Li Hu. Animate anyone: Consistent and controllable imageto-video synthesis for character animation. In *Proceedings of* the IEEE/CVF Conference on Computer Vision and Pattern Recognition, pages 8153–8163, 2024. 3
- [21] Siteng Huang, Biao Gong, Yutong Feng, Xi Chen, Yuqian Fu, Yu Liu, and Donglin Wang. Learning disentangled identifiers for action-customized text-to-image generation. In Proceedings of the IEEE/CVF Conference on Computer Vision and Pattern Recognition, pages 7797–7806, 2024. 3
- [22] Yifei Huang, Guo Chen, Jilan Xu, Mingfang Zhang, Lijin Yang, Baoqi Pei, Hongjie Zhang, Lu Dong, Yali Wang, Limin Wang, et al. Egoexolearn: A dataset for bridging asynchronous ego-and exo-centric view of procedural activities in real world. In *Proceedings of the IEEE/CVF Conference* on Computer Vision and Pattern Recognition, pages 22072– 22086, 2024. 2
- [23] Hanwen Jiang, Hao Tan, Peng Wang, Haian Jin, Yue Zhao, Sai Bi, Kai Zhang, Fujun Luan, Kalyan Sunkavalli, Qixing Huang, et al. Rayzer: A self-supervised large view synthesis model. *arXiv preprint arXiv:2505.00702*, 2025. 3

- [24] Zeyinzi Jiang, Zhen Han, Chaojie Mao, Jingfeng Zhang, Yulin Pan, and Yu Liu. Vace: All-in-one video creation and editing. arXiv preprint arXiv:2503.07598, 2025. 3
- [25] Xueyang Kang, Zhengkang Xiang, Zezheng Zhang, and Kourosh Khoshelham. Multi-view geometry-aware diffusion transformer for indoor novel view synthesis. In ICLR 2025 Workshop on Deep Generative Model in Machine Learning: Theory, Principle and Efficacy, 2025. 3
- [26] Yash Kant, Aliaksandr Siarohin, Ziyi Wu, Michael Vasilkovsky, Guocheng Qian, Jian Ren, Riza Alp Guler, Bernard Ghanem, Sergey Tulyakov, and Igor Gilitschenski. Spad: Spatially aware multi-view diffusers. In Proceedings of the IEEE/CVF Conference on Computer Vision and Pattern Recognition, pages 10026–10038, 2024.
- [27] Xin Kong, Shikun Liu, Xiaoyang Lyu, Marwan Taher, Xiaojuan Qi, and Andrew J Davison. Eschernet: A generative model for scalable view synthesis. In *Proceedings of the IEEE/CVF Conference on Computer Vision and Pattern Recognition*, pages 9503–9513, 2024. 3
- [28] Alex Krizhevsky, Ilya Sutskever, and Geoffrey E Hinton. Imagenet classification with deep convolutional neural networks. Advances in neural information processing systems, 25, 2012. 6
- [29] Insu Lee, Wooje Park, Jaeyun Jang, Minyoung Noh, Kyuhong Shim, and Byonghyo Shim. Towards comprehensive scene understanding: Integrating first and third-person views for lylms. arXiv preprint arXiv:2505.21955, 2025.
- [30] Ruilong Li, Brent Yi, Junchen Liu, Hang Gao, Yi Ma, and Angjoo Kanazawa. Cameras as relative positional encoding. arXiv preprint arXiv:2507.10496, 2025. 3
- [31] Jia-Wei Liu, Yan-Pei Cao, Jay Zhangjie Wu, Weijia Mao, Yuchao Gu, Rui Zhao, Jussi Keppo, Ying Shan, and Mike Zheng Shou. Dynvideo-e: Harnessing dynamic nerf for large-scale motion-and view-change human-centric video editing. In *Proceedings of the IEEE/CVF Conference on Computer Vision and Pattern Recognition*, pages 7664–7674, 2024. 3
- [32] Jia-Wei Liu, Weijia Mao, Zhongcong Xu, Jussi Keppo, and Mike Zheng Shou. Exocentric-to-egocentric video generation. Advances in Neural Information Processing Systems, 37:136149–136172, 2024. 1, 2, 6, 7, 8, 16
- [33] Ruoshi Liu, Rundi Wu, Basile Van Hoorick, Pavel Tok-makov, Sergey Zakharov, and Carl Vondrick. Zero-1-to-3: Zero-shot one image to 3d object. In *Proceedings of the IEEE/CVF international conference on computer vision*, pages 9298–9309, 2023. 3
- [34] Yanxing Liu, Jiancheng Pan, Jianwei Yang, Tiancheng Chen, Peiling Zhou, and Bingchen Zhang. Diverse instance generation via diffusion models for enhanced few-shot object detection in remote sensing images. *IEEE Geoscience and Remote Sensing Letters*, 2025. 3
- [35] Yanxing Liu, Jiancheng Pan, and Bingchen Zhang. Control copy-paste: Controllable diffusion-based augmentation method for remote sensing few-shot object detection. *arXiv* preprint arXiv:2507.21816, 2025. 3
- [36] Hongchen Luo, Kai Zhu, Wei Zhai, and Yang Cao. Intention-driven ego-to-exo video generation. *arXiv preprint arXiv:2403.09194*, 2024. 1, 2

- [37] Mi Luo, Zihui Xue, Alex Dimakis, and Kristen Grauman. Put myself in your shoes: Lifting the egocentric perspective from exocentric videos. In *European Conference on Com*puter Vision, pages 407–425. Springer, 2024. 2
- [38] Lorenzo Mur-Labadia, Maria Santos-Villafranca, Jesus Bermudez-Cameo, Alejandro Perez-Yus, Ruben Martinez-Cantin, and Jose J Guerrero. O-mama: Learning object mask matching between egocentric and exocentric views. In ICCV, 2025. 2
- [39] Jiancheng Pan, Shiye Lei, Yuqian Fu, Jiahao Li, Yanxing Liu, Yuze Sun, Xiao He, Long Peng, Xiaomeng Huang, and Bo Zhao. Earthsynth: Generating informative earth observation with diffusion models. *arXiv preprint arXiv:2505.12108*, 2025. 3
- [40] Jiancheng Pan, Runze Wang, Tianwen Qian, Mohammad Mahdi, Yanwei Fu, Xiangyang Xue, Xiaomeng Huang, Luc Van Gool, Danda Pani Paudel, and Yuqian Fu. V²-sam: Marrying sam2 with multi-prompt experts for cross-view object correspondence. arXiv preprint arXiv:2506.05856, 2025. 2
- [41] Junho Park, Andrew Sangwoo Ye, and Taein Kwon. Egoworld: Translating exocentric view to egocentric view using rich exocentric observations. *arXiv preprint* arXiv:2506.17896, 2025. 1, 2
- [42] William Peebles and Saining Xie. Scalable diffusion models with transformers. In *Proceedings of the IEEE/CVF inter*national conference on computer vision, pages 4195–4205, 2023, 3, 15
- [43] Chenyang Qi, Xiaodong Cun, Yong Zhang, Chenyang Lei, Xintao Wang, Ying Shan, and Qifeng Chen. Fatezero: Fusing attentions for zero-shot text-based video editing. In Proceedings of the IEEE/CVF International Conference on Computer Vision, pages 15932–15942, 2023. 3
- [44] Robin Rombach, Andreas Blattmann, Dominik Lorenz, Patrick Esser, and Björn Ommer. High-resolution image synthesis with latent diffusion models. In *Proceedings of the IEEE/CVF conference on computer vision and pattern recognition*, pages 10684–10695, 2022. 3
- [45] Nedko Savov, Naser Kazemi, Mohammad Mahdi, Danda Pani Paudel, Xi Wang, and Luc Van Gool. Exploration-driven generative interactive environments. In Proceedings of the Computer Vision and Pattern Recognition Conference, pages 27597–27607, 2025. 4
- [46] Nedko Savov, Naser Kazemi, Deheng Zhang, Danda Pani Paudel, Xi Wang, and Luc Van Gool. Statespacediffuser: Bringing long context to diffusion world models. arXiv preprint arXiv:2505.22246, 2025. 7
- [47] Yang Song, Jascha Sohl-Dickstein, Diederik P Kingma, Abhishek Kumar, Stefano Ermon, and Ben Poole. Score-based generative modeling through stochastic differential equations. arXiv preprint arXiv:2011.13456, 2020. 3
- [48] Hung-Yu Tseng, Qinbo Li, Changil Kim, Suhib Alsisan, Jia-Bin Huang, and Johannes Kopf. Consistent view synthesis with pose-guided diffusion models. In *Proceedings of the IEEE/CVF Conference on Computer Vision and Pattern Recognition*, pages 16773–16783, 2023. 3
- [49] Team Wan, Ang Wang, Baole Ai, Bin Wen, Chaojie Mao, Chen-Wei Xie, Di Chen, Feiwu Yu, Haiming Zhao, Jianxiao

- Yang, et al. Wan: Open and advanced large-scale video generative models. *arXiv preprint arXiv:2503.20314*, 2025. 1, 12, 13
- [50] Daniel Watson, William Chan, Ricardo Martin-Brualla, Jonathan Ho, Andrea Tagliasacchi, and Mohammad Norouzi. Novel view synthesis with diffusion models. arXiv preprint arXiv:2210.04628, 2022. 3
- [51] Jay Zhangjie Wu, Yixiao Ge, Xintao Wang, Stan Weixian Lei, Yuchao Gu, Yufei Shi, Wynne Hsu, Ying Shan, Xiaohu Qie, and Mike Zheng Shou. Tune-a-video: One-shot tuning of image diffusion models for text-to-video generation. In *Proceedings of the IEEE/CVF international conference on computer vision*, pages 7623–7633, 2023. 3
- [52] Jilan Xu, Yifei Huang, Baoqi Pei, Junlin Hou, Qingqiu Li, Guo Chen, Yuejie Zhang, Rui Feng, and Weidi Xie. Egoexogen: Ego-centric video prediction by watching exo-centric videos. *arXiv preprint arXiv:2504.11732*, 2025. 1, 2
- [53] Zhongcong Xu, Jianfeng Zhang, Jun Hao Liew, Hanshu Yan, Jia-Wei Liu, Chenxu Zhang, Jiashi Feng, and Mike Zheng Shou. Magicanimate: Temporally consistent human image animation using diffusion model. In *Proceedings of the IEEE/CVF Conference on Computer Vision and Pattern Recognition*, pages 1481–1490, 2024. 3
- [54] Zhuoyi Yang, Jiayan Teng, Wendi Zheng, Ming Ding, Shiyu Huang, Jiazheng Xu, Yuanming Yang, Wenyi Hong, Xiaohan Zhang, Guanyu Feng, et al. Cogvideox: Text-to-video diffusion models with an expert transformer. *arXiv preprint arXiv:2408.06072*, 2024. 3
- [55] David Junhao Zhang, Jay Zhangjie Wu, Jia-Wei Liu, Rui Zhao, Lingmin Ran, Yuchao Gu, Difei Gao, and Mike Zheng Shou. Show-1: Marrying pixel and latent diffusion models for text-to-video generation. *International Journal of Computer Vision*, 133(4):1879–1893, 2025. 3
- [56] Daquan Zhou, Weimin Wang, Hanshu Yan, Weiwei Lv, Yizhe Zhu, and Jiashi Feng. Magicvideo: Efficient video generation with latent diffusion models. arXiv preprint arXiv:2211.11018, 2022. 3



Solution Exo2EgoSyn: Unlocking Foundation Video Generation Models for **Exocentric-to-Egocentric Video Synthesis**

Supplementary Material

Contents 1 1. Introduction 2 2. Related Works 2 2.1. Ego-exo Cross-view Learning 3 3. Methodology 3 4 3.3. EgoExo-Align Module 4 3.4. Relaxing Novel Conditions 4 3.4.1 . Multi-view Exocentric Video Condi-5 5 3.4.2 . Pose-Aware Latent Injection 3.5. Training and Loss Functions 5 4. Experiments 5 5 4.1. Experimental Setup 4.2. Comparison with Baseline 6 5. Conclusion 8 6. Biases in Video Foundation Models 12 7. Impact of the EgoExo-Align Module 12 12 8. Training Setup and Hyperparameters 12 8.1.1 . EgoExo-Align Module 12 8.1.2 . WAN2.2 VAE 13 8.1.3 . WAN2.2 Transformer 15 8.2.1 . EgoExo-Align Module 15 8.2.2 . MultiExoCon Module 15 8.2.3 . PoseInj Module 15 16 9. User Study Materials 10Additional Qualitative Visualizations **16** 11Analysis of Failure Modes 16 12Future Work 16

6. Biases in Video Foundation Models

As outlined in the Introduction, obstacle ①: Strong view bias, and in Section 3.2 (Our Framework), foundation video generative models tend to reproduce the conditioned image as the first frame of the generated video. This behavior significantly complicates our goal of cross-view generation. In this section, we present examples demonstrating how the WAN2.2 [49] model consistently prioritizes the conditioned image over the conditioned text—even in cases where we explicitly prompt the model to avoid replicating the first frame. We first examine this effect using general, non-task-specific text prompts, and then with ego-centric prompts tailored to our setting. Across all cases, the model exhibits a strong bias toward preserving the first frame, indicated by red in Fig. 5.

7. Impact of the EgoExo-Align Module

Our ablation studies (Section 4.3, Table 2) confirm the necessity of the EgoExo-Align module, as its removal causes a significant performance drop. An upper performance bound is established when the model is provided with the groundtruth first frame from the ego-view video. To further isolate this module's contribution, we applied EgoExo-Align in a frame-by-frame manner (Fig. 6, last row). The resulting poor performance demonstrates that, while necessary, the module is insufficient on its own and produces blurry outputs. It is the subsequent fine-tuning with WAN2.2 that is critical for transforming this initial alignment into a highquality video, confirming their synergistic relationship.

8. Training Setup and Hyperparameters

In this section, we first describe the architecture of the EgoExo-Align module, the WAN2.2 VAE, and the WAN2.2 denoising transformer. Subsequently, we provide the specific training parameters for each stage of the pipeline.

8.1. Models

8.1.1. EgoExo-Align Module

Our EgoExo-Align module is implemented as a non-causal STTransformer [6], with the hyperparameters in Table 7. Attention is applied in a sequential order: first spatial, then temporal. The module produces 22 output channels, of which 16 correspond to latent VAE features and 6 to Plücker embeddings. Within the architecture, we employ the Posi-

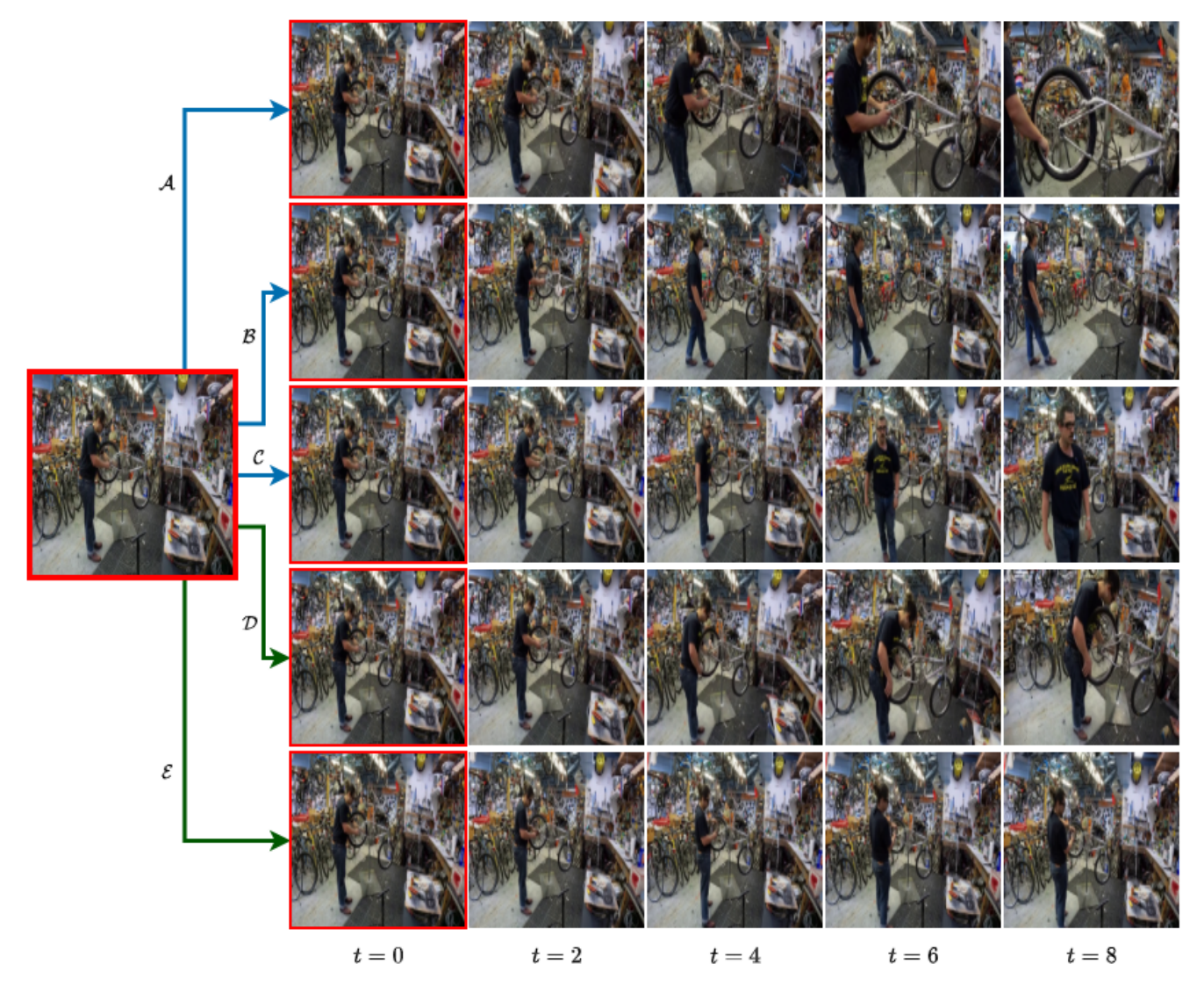


Figure 5. **WAN2.2's Bias of Replicating the Conditioned Image.** On the left is the conditioning image. On the right, WAN2.2 generates five distinct videos based on different text prompts. The first three (blue arrows) use general prompts, while the last two (green arrows) use prompts tailored for our task. The text prompts used are as follows: \underline{A} : "Do start the video from a black frame.", $\underline{\mathcal{B}}$: "Begin the video at a moment when the man is already in motion farther down the bike, as if some time has passed since the moment shown in the image.", $\underline{\mathcal{C}}$: "The video must not begin with a scene resembling the supplied image. The opening frame should show a noticeably changed situation — the man in a different location or pose.", $\underline{\mathcal{D}}$: "Produce a fully ego-centric video starting from the provided image. The camera must be strictly from the man's eyes, showing the environment as he sees it — hands, body, and movement should appear naturally from a first-person perspective.", and $\underline{\mathcal{E}}$: "Generate the ego-centric video from the image.".

tion Encoding Generator (PEG) [7] in its non-causal configuration.

8.1.2. WAN2.2 VAE

WAN2.2 provides five main sets of pre-trained weights:

- *T2V-A14B*: Text2Video Mixture-of-Experts(MoE) model which supports 480/720P video generation.
- *I2V-A14B*: Image2Video MoE model which supports 480/720P video generation.
- TI2V-5B: T2V+I2V, using high-compression VAE which

supports 720P video generation.

- *S2V-14B*: Speech2Video model which supports 480/720P video generation.
- Animate-14B: character animation and replacement.

The first two models use the VAE from WAN2.1 [49], while the third introduces a new VAE with higher spatiotemporal compression. As defined in Section 3.1, the compression factors (c_f, c_h, c_w) are (4, 8, 8) for the first two setups and (4, 16, 16) for the third. In this work, we use the

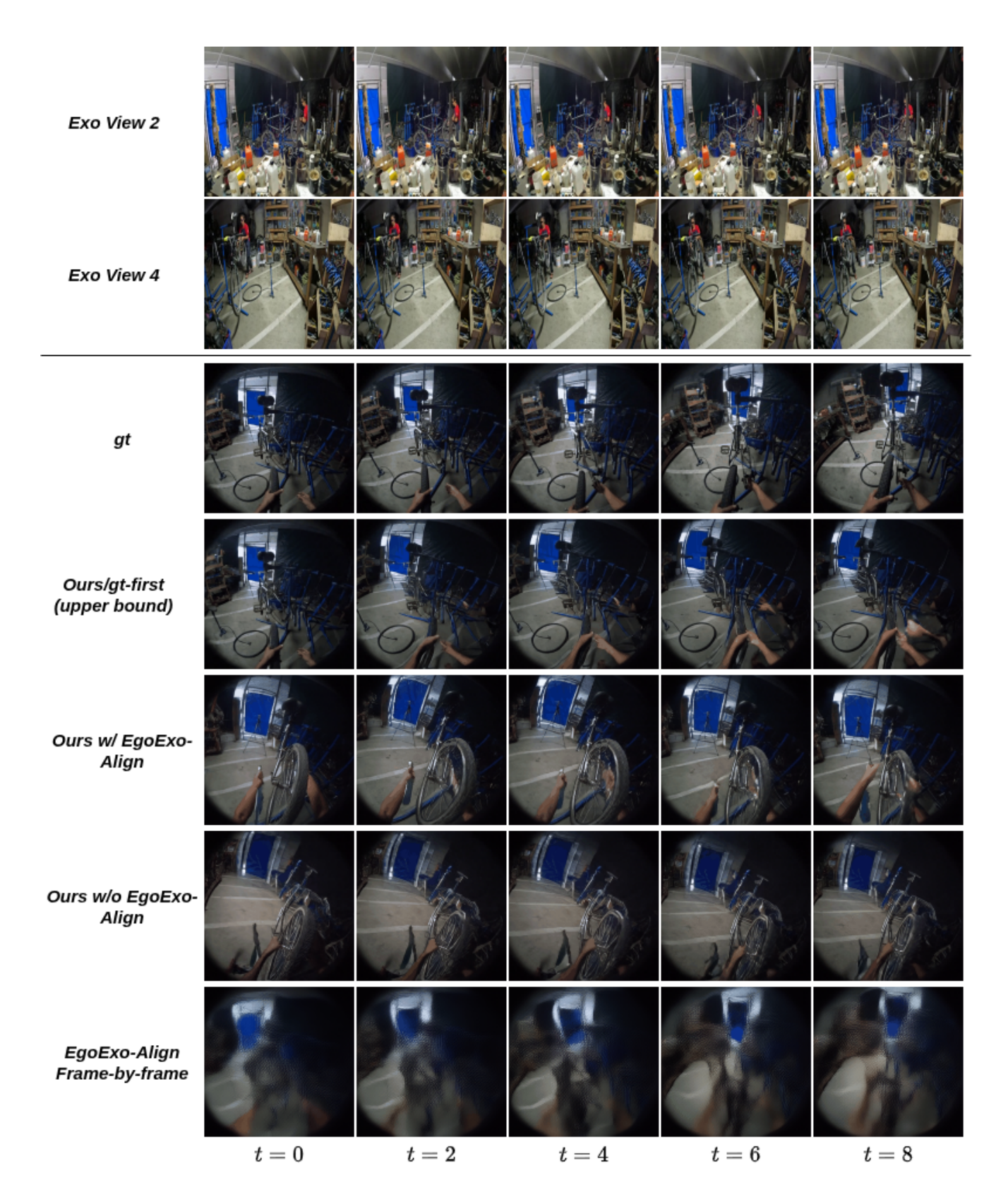


Figure 6. **EgoExo-Align Module.** Top: Model inputs. The second and fourth exo videos are shown for illustration, appearing in the first and second rows, respectively. Bottom: The second row presents an upper-bound performance by conditioning Exo2EgoSyn on a ground-truth ego-view first frame. A comparison between the third and fourth rows—with and without the EgoExo-Align module, respectively—confirms the module's necessity. Conversely, the last row, which results from applying the module in a standalone, frame-by-frame manner, demonstrates its insufficiency. This contrast highlights that effective synthesis requires both the EgoExo-Align module and the subsequent fine-tuning of the WAN2.2 model (third row).

Parameter	Value			
STTransformer				
Out channels	22			
Dim	512			
Heads	8			
Num blocks	8			
Dim head	64			
FF multiplier	4.0			
Attn dropout	0.0			
FF dropout	0.0			

Table 7. Hyperparameters of the EgoExo-Align Module.

Parameter	Value
VAE	
VAE Kind	Wan2.1_VAE
VAE stride	(4, 8, 8)
Transformer	
Patch size	(1, 2, 2)
Dim	5120
FFN dim	13824
Freq dim	256
Num heads	40
Num DiT blocks	40
QK norm	True
Cross-attn norm	True
Epsilon	1×10^{-6}
Total timesteps	1000
Inference	
Sample shift	5.0
Boundary (θ)	900
Sample guide scale	3.5
Inference steps	40

Table 8. Configuration of the Denoising Transformer.

I2V-A14B model, which employs the VAE with parameters $c_f=4,\,c_h=8,\,c_w=8$. This VAE is frozen during all experiments and contains 127M parameters.

8.1.3. WAN2.2 Transformer

As previously stated, our work is based on the I2V-A14B model. This model employs a mixture of two experts: a high-noise transformer for denoising at timesteps $t>\theta$ (low SNR) and a low-noise transformer for timesteps $t\le\theta$ (high SNR). The value of $\theta=900$ in the actual implementation. These two experts are identical in architecture, each having 14B parameters. We use only the low-noise transformer for all experiments in this work. The hyperparameters used for the transformer are detailed in Table 8.

8.2. Training

8.2.1. EgoExo-Align Module

We train the STTransformer model, which has 50M parameters, using the training configurations listed in Table 9.

Parameter	Value
Core Training	
Train batch size	128
Mixed precision	bf16
Max grad norm	1.0
Loss function	L1
Views (exo)	4
Optimization	
Learning rate	1×10^{-4}
Scheduler	cosine
Warmup steps	200
Min learning rate	5×10^{-5}
Optimizer	Adam
Weight decay	1×10^{-4}
Adam ϵ	1×10^{-8}
Adam betas	(0.9, 0.95)

Table 9. Training parameters of the EgoExo-Align Module.

8.2.2. MultiExoCon Module

The objectives for this fine-tuning stage are twofold: first, to enable a holistic understanding of the environment from the multi-view exocentric inputs, and second, to learn camera motion implicitly from the visual dynamics of the frames, without relying on explicit camera poses:

$$\mathcal{L}_2 = \left\| \epsilon_t - \mathcal{W} \left([z_t, \hat{l}_1^{\mathrm{ego}}], \mathcal{V}^{\mathrm{exo}}, t \right) \right\|^2.$$

As outlined in the paper (Line 335), when conditioning on four exocentric videos, the detached output of the EgoExo-Align module (\hat{l}_1^{ego}) serves as the consistent input to the diffusion model. We detail the training setup for this stage in Table 10. In this stage, we train all cross-attention parameters in each DiT [42] block, while using LoRA [19] to fine-tune only the self-attention modules. The LoRA components introduce 210M trainable parameters. For the inference stage, we follow the same configuration settings described in Table 8.

8.2.3. PoseInj Module

This fine-tuning stage aims to improve camera motion tracking through the explicit use of relative camera poses:

$$\mathcal{L}' = \left\| \epsilon_t - \mathcal{W}([z_t, \hat{l}_1^{\text{ego}}, E(P^{rel}, K)], \mathcal{V}^{\text{exo}}, t) \right\|^2.$$

To achieve this, we provide the training pipeline with an additional condition: the Plücker embedding of relative poses, adhering to the training configuration detailed in Table 10. In this stage, we use LoRA to fine-tune only the self-attention modules. The LoRA components introduce 210M trainable parameters. For the inference stage, we follow the same configuration settings described in Table 8.

Setting	Value
LoRA rank	128
LoRA alpha	128
Precision	bf16
Exo size $(H \times W)$	256×256
Ego size $(H \times W)$	256×256
FPS	3
Frames	9
Batch size	3
Training steps	100000
Grad. accumulation	1
Learning rate	1×10^{-4}
Min learning rate	5×10^{-5}
LR scheduler	cosine
Warmup steps	200
LR cycles	1
Optimizer	Adam (8-bit)
Weight decay	1×10^{-4}
Adam ϵ	1×10^{-8}
Adam β_1	0.9
Adam β_2	0.95
Max grad norm	1.0

Table 10. **Training Setup.** Both the first (MultiExoCon module) and second (PoseInj module) fine-tuning stages use the same training setup, differing only in the set of trainable parameters.

9. User Study Materials

We provide additional details on our user study, which evaluates the proposed Exo2EgoSyn model in comparison to the baseline VAWAN. In Fig. 7 we show the interface for a single sample given to the user. A clip is shown with two parts, which the user should compare and rate. The order of the samples is random. The instructions given to the users at the start of the study are provided below:

Thank you for taking part in our user study! For each question you will see a row of 3 video frames. The reference video is outlined in grey. The two candidate video frames are outlined in blue and red.

Grey Video Frames: Ground-truth reference.

<u>Blue</u> Video Frames: Candidate that attempts to resemble the grey reference frames.

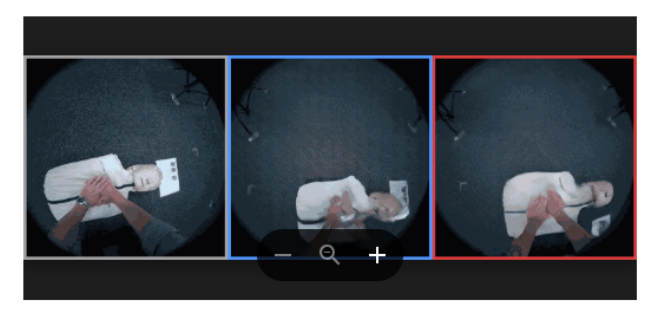
<u>Red</u> Video Frames: Candidate that attempts to resemble the grey reference frames.

There are 100 samples in total. For each sample, decide which candidate most closely matches the content of the grey reference frames. Please base your decision on the accuracy of the hand-over-object interaction, the visual quality, and the camera motion tracking.

Options:

BLUE: The blue video resembles the grey video better RED: The red video resembles the grey video better NONE: Both options equally well represent the grey After rating all sequences, click "Submit" to record your

Sample 33



Which image matches better the grey bordered image:



Figure 7. User Study Sample.

responses. Your feedback is invaluable—thank you!

As outlined in Section 4.2, we conducted a user study with 10 participants who cast a total of 919 votes. The results show a clear preference for our model, which received 515 votes, compared to 215 votes for "None" and 189 votes for the VAWAN baseline.

10. Additional Qualitative Visualizations

Extending the qualitative analysis in the paper, we present further visual comparisons for all categories in our evaluation. Fig. 8, Fig. 9, Fig. 10, and Fig. 11 illustrate example outputs from the Bike, Basketball, CPR, and Covid Test categories, respectively, demonstrating the performance of our proposed model against the baseline.

11. Analysis of Failure Modes

An analysis of our model's limitations reveals specific failure modes. Performance degrades primarily when the EgoExo-Align module produces a poor initial frame prediction, or when the predicted frame, while semantically correct, lacks informative visual content to guide the subsequent generation. For instance, an accurately predicted but textureless image of a basketball court floor provides insufficient cues for the model to generate a meaningful subsequent action. Failures also occur during actions with very fast motion, leading to blur in the egocentric view. Fig. 12 visualizes examples of these failure cases.

12. Future Work

Although prior work [32] has begun exploring pretrained models (a 2D image generative U-Net adapted from Stable Diffusion [4]) for exocentric-to-egocentric generation, these methods are not built upon foundation-scale video generative models. Instead, they typically rely on a two-stage pipeline: a frame-to-frame generation model is trained first,

and a motion module is later finetuned to stitch individual frames into a coherent sequence. In contrast, we are the first to build on a foundation video model and generate the full video frames at once, adhering to the principles and capabilities of modern large-scale video generation.

However, generating the full video at once introduces a notable challenge: precise frame-level alignment of camera motion. While our model reliably captures the overall camera trajectory (e.g., a left-to-right sweep), it may shift the exact frame where a directional change occurs, for example, executing a turn slightly before or after the ground-truth frame t. This behavior is an inherent consequence of holistic sequence generation. Methods that operate frame-by-frame, followed by temporal stitching, naturally maintain strict per-frame motion cues, which our onepass approach does not explicitly enforce. Thus, a promising direction for future work is to augment our singlepass foundation-model pipeline with mechanisms that enable accurate, frame-specific adherence to camera pose transitions-without reverting to frame-by-frame prediction. Achieving such fine-grained temporal alignment while preserving the advantages of full-sequence generation represents an important next step toward robust and precise cross-view video synthesis.

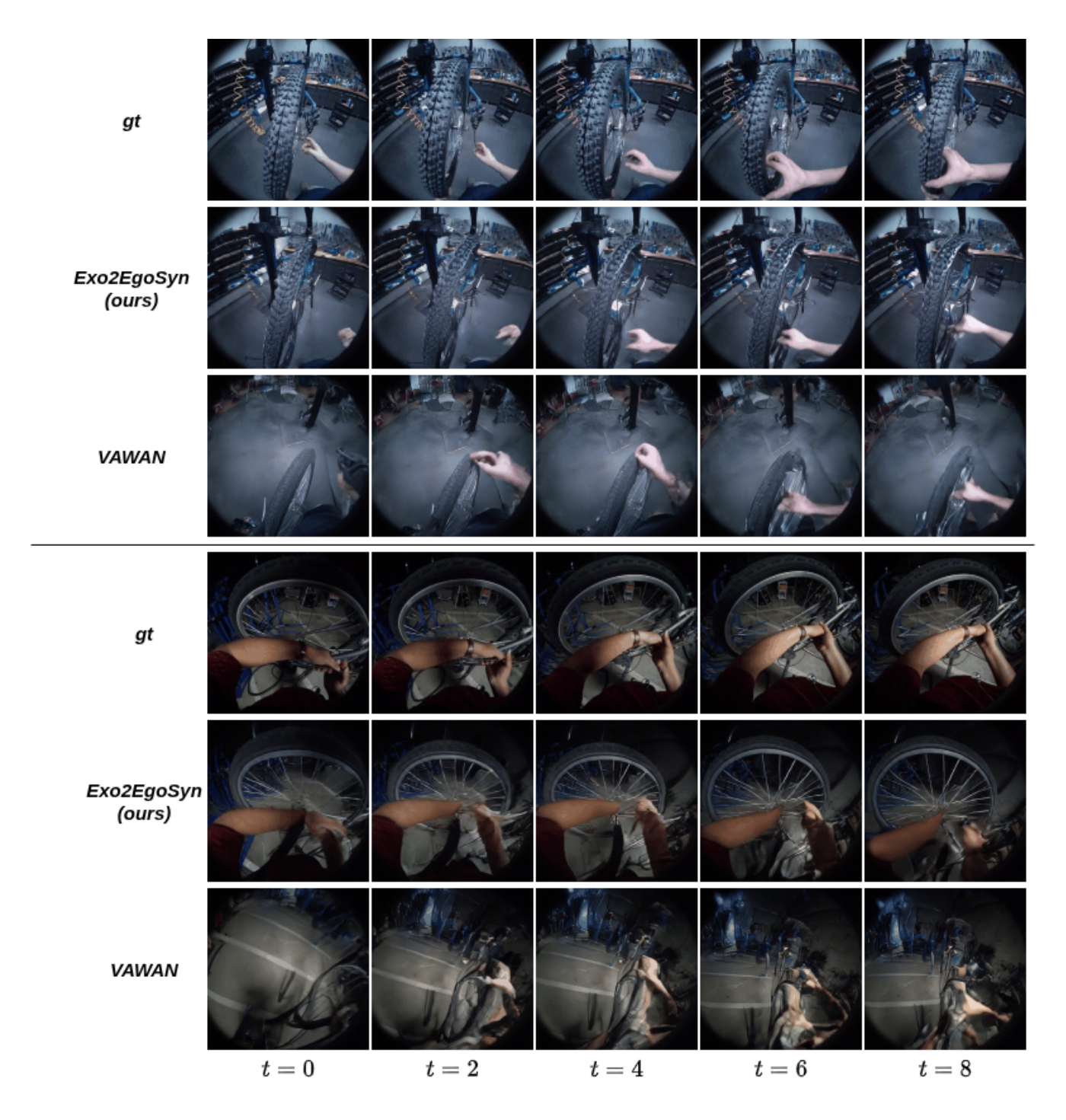


Figure 8. **Qualitative Results.** Bike.

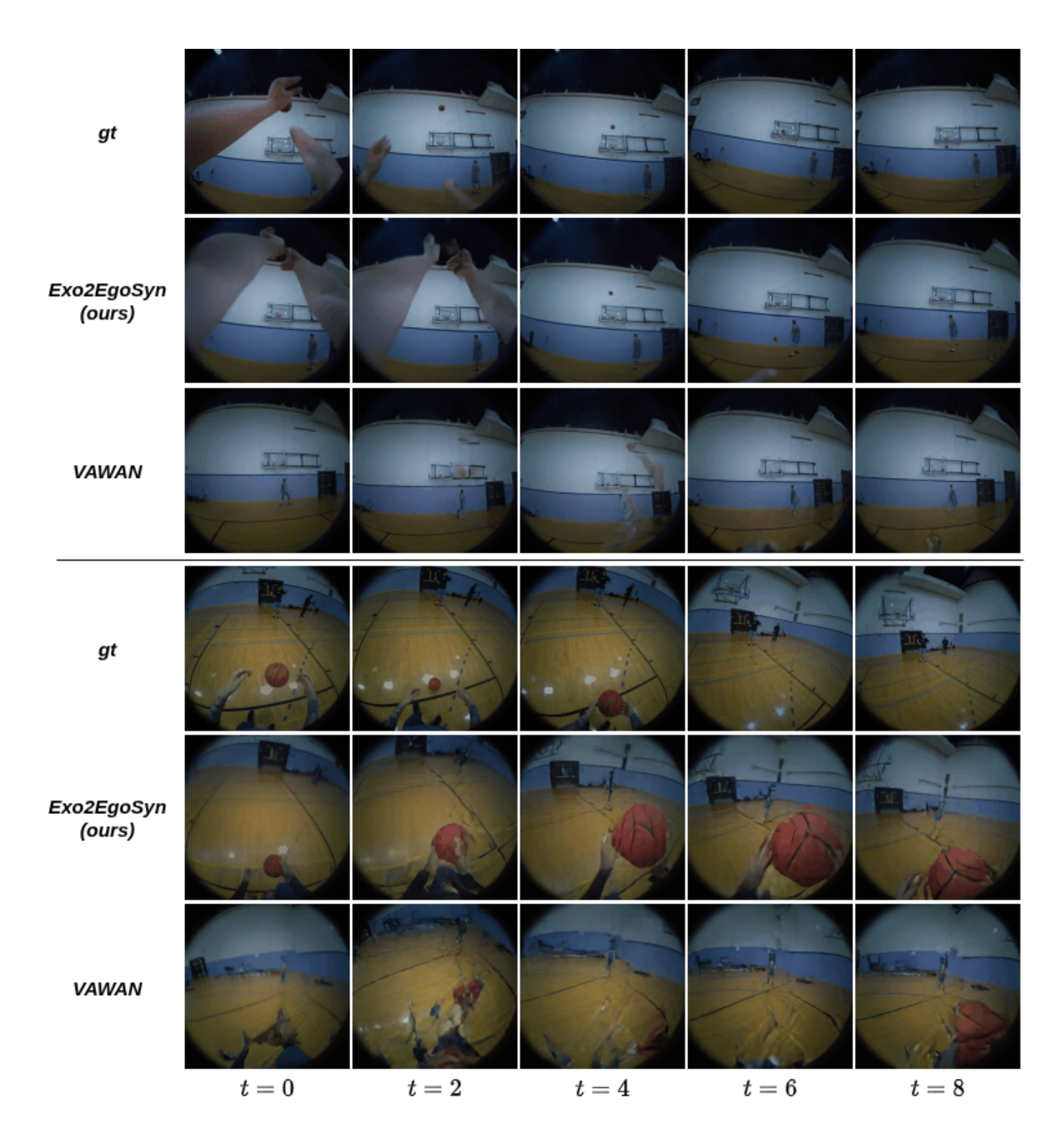


Figure 9. **Qualitative Results.** Basketball.

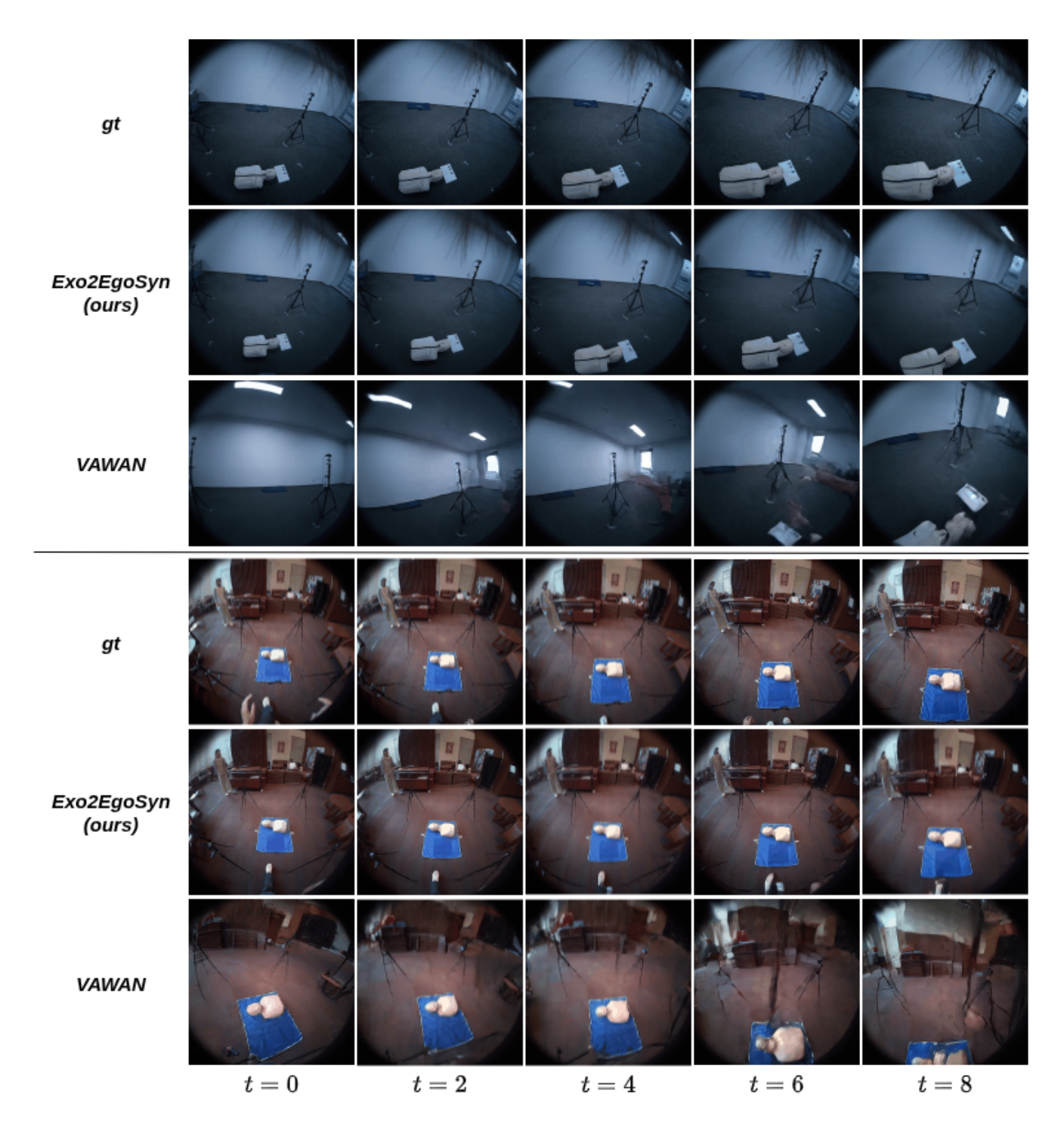


Figure 10. **Qualitative Results.** CPR.

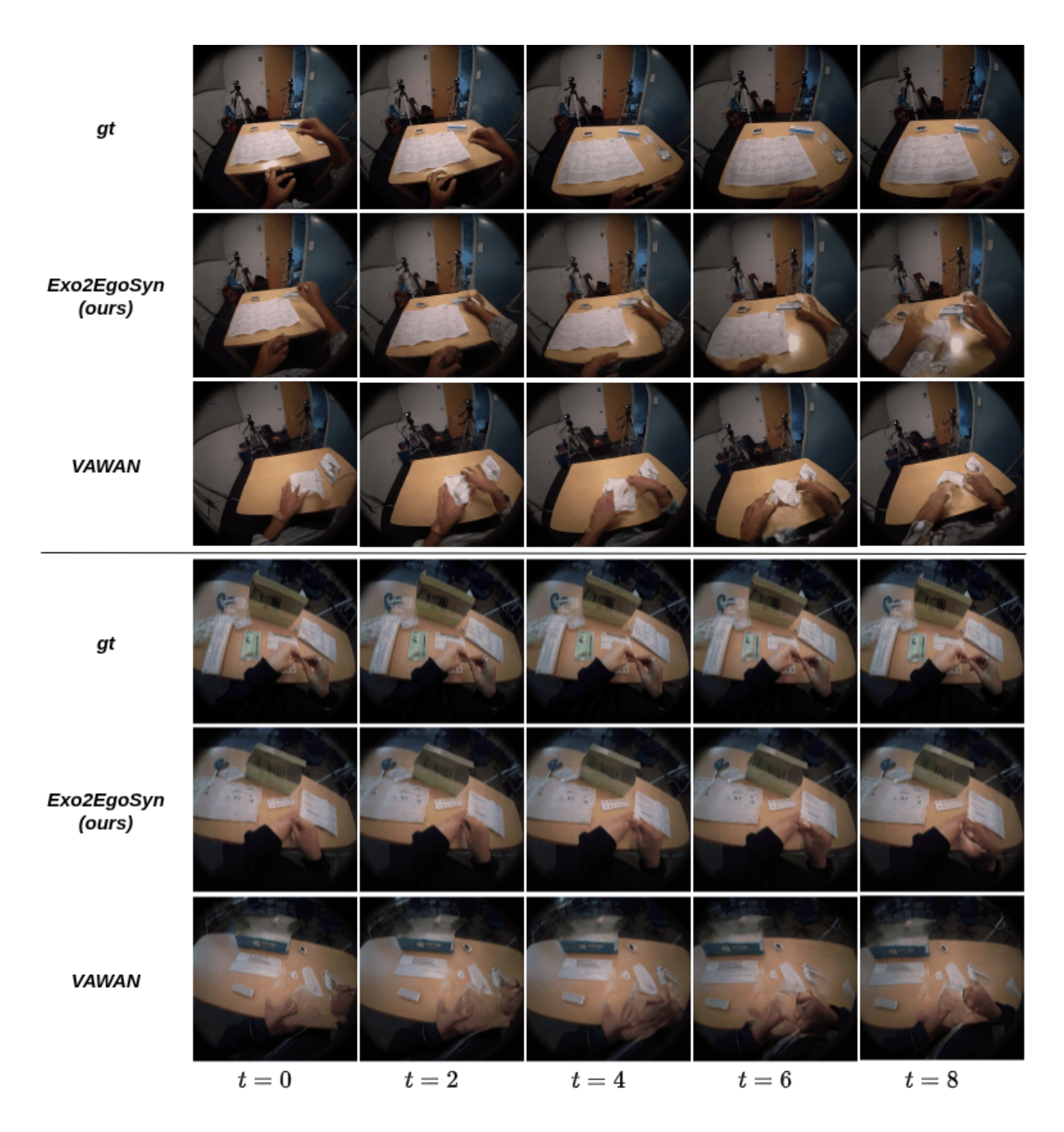


Figure 11. **Qualitative Results.** Covid Test.

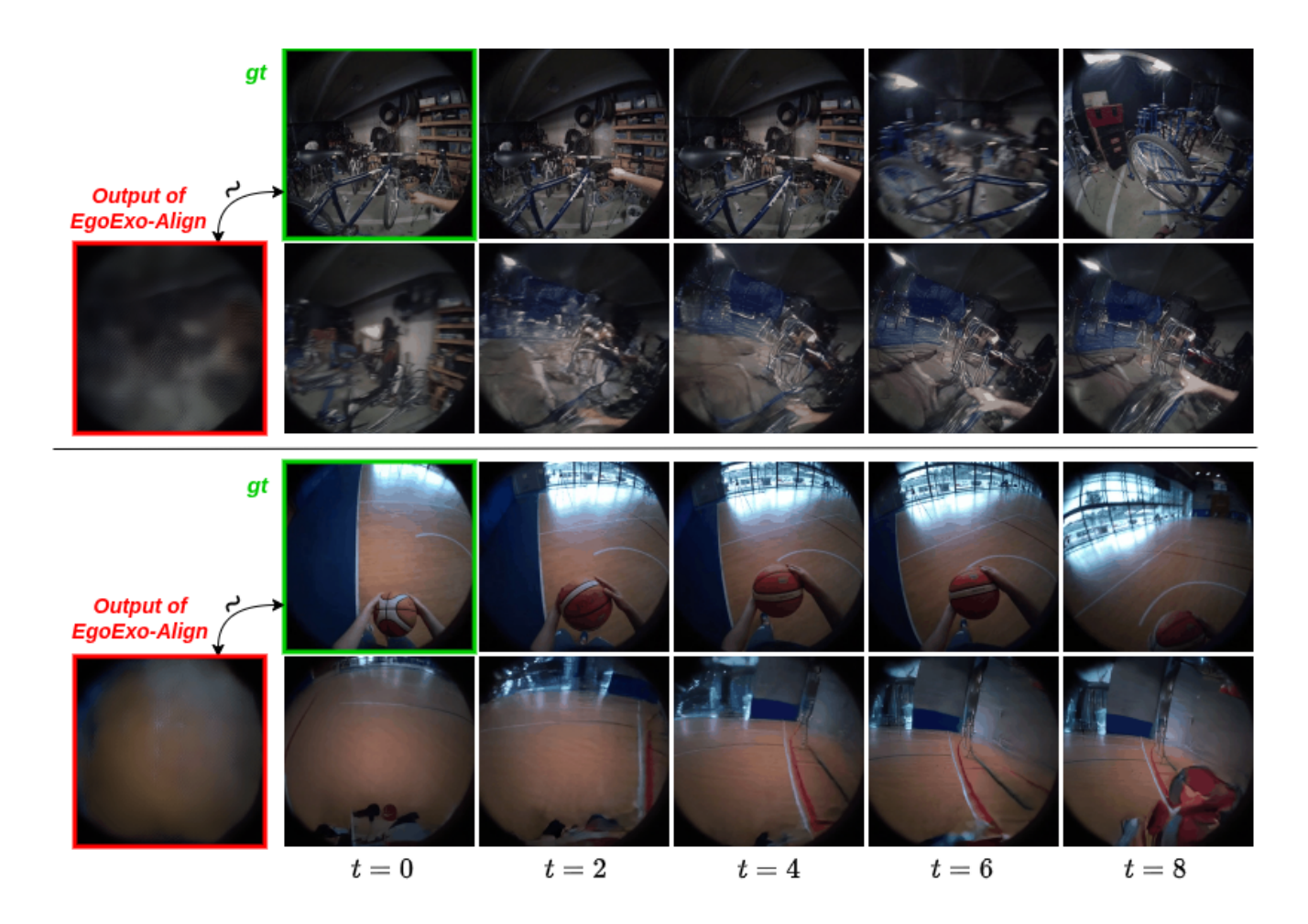


Figure 12. **Failure Cases.** Top: A case where the EgoExo-Align output (red) fails to accurately reconstruct the first frame of the ego video (green). This initial misalignment, combined with fast camera motion in the ground-truth sequence (see t=6), causes the model to produce poor results. Bottom: Here, EgoExo-Align produces a textureless conditioning frame. While the model successfully mimics the camera motion (compare predicted and ground-truth rows), it fails to generate the essential elements of the scene, namely the ball and the detailed basketball court.